

# Experimental and numerical analysis on normalization of picture frame tests for composite materials

X.Q. Peng<sup>a</sup>, J. Cao<sup>a,\*</sup>, J. Chen<sup>b</sup>, P. Xue<sup>a</sup>, D.S. Lussier<sup>b</sup>, L. Liu<sup>b</sup>

<sup>a</sup>Northwestern University, Department of Mechanical Engineering, Evanston, IL 60208, USA

<sup>b</sup>University of Massachusetts, Lowell, Department of Mechanical Engineering, Lowell, MA 01854, USA

Received 27 August 2002; received in revised form 8 April 2003; accepted 13 April 2003

## Abstract

Material characterization of woven fiber reinforced composites is one of the critical issues in promoting their applications. Existing experimental tests for characterizing the material behavior of textile composites include the shear frame test, biaxial tensile test and bias extension test. Each test method has its own merits as well as its disadvantages. One important question is how to correlate testing data from different laboratories, specifically, how to compare the data? Should we normalize the reaction force by the side length or by the area of the composite sheet in the shear frame test? In this paper, we discuss this question from the energy point of view with the assistance of numerical simulations, and present experimental results designed to address this problem. Our answer to this question is 'it depends', i.e., how to normalize the data depends on the experimental configuration.

© 2003 Elsevier Ltd. All rights reserved.

*Keywords:* Plain weave composites

## 1. Introduction

Woven fiber reinforced composites have demonstrated their great potential as a viable alternative to metal sheet for high-strength and low-weight products. Over the past several years, many studies have been conducted on the material behavior and the forming process of these composites. As there are immense varieties of available composite materials, possible fabric construction geometry, and changes in composite material properties during processing, an efficient design approach is desired. Numerical simulations can be powerful tools to improve the viability of the manufacturing processes for woven composites, by the optimization of process parameters, materials selection, and tooling design. As known, all simulations require the input of a proper material constitutive law and the associated parameters. Unfamiliarity with the material behavior can lead to defects such as wrinkling, tearing and bridging. This makes standard material testing methods essential to understanding the effects of material and

process variables (e.g., weave pattern, temperature, rate, binder pressure) on formability, and to providing input data and validation data for numerical simulations.

Material test methods for woven composites reported in the literature include bi-axial tensile tests, bias extension tests and shear frame tests [1–13]. The bi-axial tensile tests can predict the extension behavior along the yarn direction of the composite. The normalization of this test is straightforward, i.e., force divided by the cross-section area. In the forming operation, the fabric yarns also experience large angular variation between weft and warp yarns. Hence, here in this paper, we will mainly focus on the tests for this shear behavior of woven composites.

Two experimental approaches can be used to characterize the shear behavior of woven composites: the bias extension test [2–7] and the shear frame test [8–13]. The bias extension test is essentially a uni-axial extension test with the dimension of the test sample in the loading direction relatively greater than the width, and the yarns initially oriented at  $\pm 45^\circ$  to the loading direction. It is favored by a number of researchers due to the simplicity of the experimental procedure. However, the bias extension approach usually brings out a complex combination of shear and tension, which

\* Corresponding author. Tel.: +1-847-467-1032; fax: +1-847-491-3915.

E-mail address: [jcao@northwestern.edu](mailto:jcao@northwestern.edu) (J. Cao).

makes it difficult to isolate the shear deformation in the test and hence complicates the characterization of pure shear behavior of textile composites.

In the shear frame test, a composite sheet is clamped within a square frame hinged at each corner. The two diagonally opposite corners are then displaced using a mechanical testing machine. Compared to the bias extension test, the shear frame test requires a more complex experimental set-up. However, it can produce a quite uniform shear deformation state in the composite sheet. Hence, in our opinion, the shear frame test is a better way to obtain the pure shear behavior of woven composites, and this test will be the focus of the work presented here.

Different laboratories may have different shear frame sizes. Even with the same shear frame, various test samples can be obtained by having different cut-off areas at the four corners of the fabric. One question then arises: how do we compare and interpret the experimental results for the same woven composite material with the same woven pattern under various circumstances? To be more precise, how should we normalize the experimental data, since the material properties at this scale should be independent of any testing methods and testing apparatus? Should we normalize the data by the composite sheet edge length or by the fabric area being sheared or by the number of crossovers in the fabric? The answer to this question is crucial because it will determine the necessary input data of material properties for future numerical simulations and further optimization of forming processes.

Taking plain weave composites as an example, we will first address this issue analytically from the energy point of view. Then numerical shear frame tests will be conducted on a unit-cell representing the plain weave composite as well as on an expanded unit-cell by displacing diagonally. The resulting reaction forces are normalized by both the edge lengths of the unit-cells and their areas. Comparisons of normalized force versus shear angle curves are used to strengthen the conclusion obtained from the energy approach. In Section 4, full size shear frame tests of plain weave composite sheets are simulated using shell elements. The equivalent material properties for the shell elements are obtained from a material characterization approach proposed by the authors in [14,15]. The results are again normalized by two ways and compared to provide further support for our answer to the normalization issue. Section 5 presents experimental data of shear frame tests on the same plain weave composite. Phenomena observed in the experiments are explained and the results support our theoretical analysis. Section 6 provides the discussion on the normalizations by combining the simulation results and experimental data. Finally, conclusions are stated in Section 7.

## 2. Energy approach for normalization

For the purpose of this normalization study, shear frame tests can be theoretically carried out with two different experimental set-ups. One set-up is to have full-size composite fabrics clamped in shear frames with different sizes (we will therefore call it set-up I, see Fig. 1.). Another set-up (set-up II) is to use the same shear frame but fabrics with a different corner cut-off area, as shown in Fig. 2. Normalization will be first investigated by energy analysis on these two experimental set-ups.

For set-up I, suppose composite patches are clamped in two shear frames with different frame lengths,  $L_{\text{frame}}$  and  $l_{\text{frame}}$ , respectively, and  $L_{\text{frame}} > l_{\text{frame}}$ , as shown in Fig. 1. The forces  $P$  and  $p$  act, respectively, on points  $A$  and  $a$  and the work done,  $W$  and  $w$ , can be expressed as

$$W = \int P d\Delta = \bar{P} \Delta_P \quad (1)$$

$$w = \int p d\delta = \bar{p} \delta_p \quad (2)$$

where  $\Delta$  and  $\delta$  are the displacements at the loading points  $A$  and  $a$ , respectively.  $\Delta_P$  and  $\delta_p$  are the final displacements at the loading points  $A$  and  $a$  in the vertical direction. The work done by the external forces  $P$  and  $p$  will transfer to strain energies, which contributes mostly to the shear deformation of the composite sheets. A larger fabric area is constructed of many more yarns,

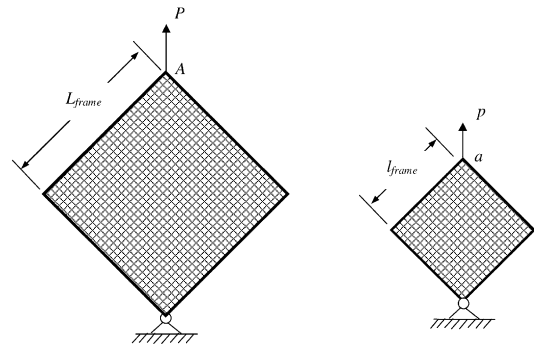


Fig. 1. Full composite sheets in different shear frames (set-up I).

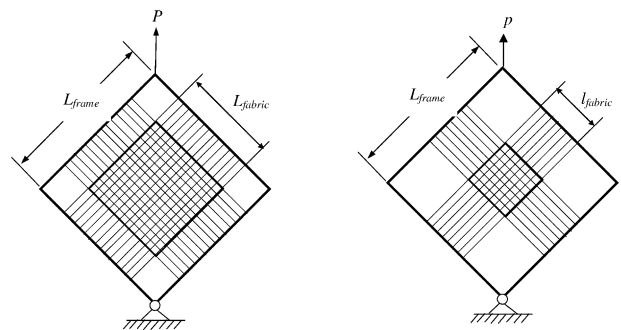


Fig. 2. Composite sheets with corner cut-offs in same shear frame (set-up II).

causing more crossovers within the composite patch. More crossovers would increase the friction and compaction loads needed for yarn rotation. Consequently, it is justified on the basis of energy that the work done per unit volume should be a constant,  $\beta$ , which is independent of the length of the composite patch, namely

$$\frac{W}{A_L T} = \frac{w}{A_l t} = \beta \quad (3)$$

where  $A_L$  and  $A_l$  are the areas, and  $T$  and  $t$  are the thicknesses of the composite patches.

Assuming  $T = t$  since the same woven composite materials are considered and combining Eqs. (1)–(3), the relation can be written as

$$\frac{W}{w} = \frac{\bar{P}\Delta_P}{\bar{p}\delta_p} = \frac{A_L}{A_l} = \frac{L_{\text{fabric}}^2}{l_{\text{fabric}}^2} \quad (4)$$

where  $L_{\text{fabric}} = L_{\text{frame}}$  and  $l_{\text{fabric}} = l_{\text{frame}}$  in set-up I. On the other hand, the displacements at the loading points,  $A$  and  $a$ , can be calculated from the geometric analysis assuming that the shear strain distributes evenly under the trellising shear tests. From Fig. 3, we have

$$\delta_p = l_{\text{frame}}[2\cos(\pi/4 - \theta/2) - \sqrt{2}] \quad (5)$$

$$\Delta_P = L_{\text{frame}}[2\cos(\pi/4 - \theta/2) - \sqrt{2}] \quad (6)$$

In Eqs. (5) and (6),  $\theta$  is the shear angle of the composite patch in the trellising shear test. At the same shear deformation level, the displacements are proportional to the length of the composite patch. Consequently, we have

$$\frac{\delta_p}{l_{\text{frame}}} = \frac{\Delta_P}{L_{\text{frame}}} \quad (7)$$

Substituting Eq. (7) into Eq. (4), it can be obtained that

$$\frac{\bar{P}}{\bar{p}} = \frac{L_{\text{frame}}^2 \delta_p}{l_{\text{frame}}^2 \Delta_P} = \frac{L_{\text{frame}}}{l_{\text{frame}}} \quad (8)$$

Therefore, in set-up I, the load should be normalized by the length of the patch, not the area, based on this analysis.

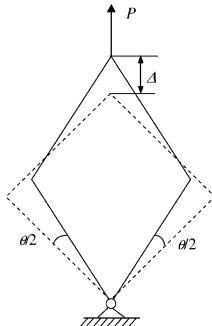


Fig. 3. Deformed composite sheet in shear frame tests.

In set-up II, composite fabrics with different corner cut-offs are clamped in the same shear frame with a frame size as  $L_{\text{frame}}$ , as illustrated in Fig. 2. The four arm parts of the fabric considered here are not woven structures, i.e., no crossovers. Hence, as a reasonable approximation, the work done by the pulling force is considered to fully contribute to the trellising deformation of the central square part. Consequently, Eqs. (1)–(4) still hold for set-up II. However, in contrast to Eq. (7) for set-up I, when two composite patches experience the same shear angle level,  $\theta$ , we have in set-up II that

$$\delta_p = \Delta_P \quad (9)$$

Substituting Eq. (9) into Eq. (4), it can be obtained that

$$\frac{\bar{P}}{\bar{p}} = \frac{L_{\text{fabric}}^2 \delta_p}{l_{\text{fabric}}^2 \Delta_P} = \frac{L_{\text{fabric}}^2}{l_{\text{fabric}}^2} \quad (10)$$

Now the load in set-up II should be normalized by the area of the patch instead of the length, as can be seen from Eq. (10). Combining with the result from set-up I, we can conclude that the normalization of load in shear frame tests depends on the experimental set-up. Length normalization should be used in set-up I and area normalization is for set-up II. The essential difference between the two set-ups is that the shear frame size can be considered equal to the composite patch size in set-up I, while in set-up II, the frame size is much larger than the patch size and the contributions from the arm area to the load force are assumed to be negligible.

For more general cases of comparing results from different specimen sizes and different frame sizes, the ratio of the loads can be expressed as

$$\frac{\bar{P}}{\bar{p}} = \frac{L_{\text{fabric}}^2/L_{\text{frame}}}{l_{\text{fabric}}^2/l_{\text{frame}}} \quad (11)$$

which simplifies to set-up I if  $L_{\text{fabric}} = L_{\text{frame}}$  and  $l_{\text{fabric}} = l_{\text{frame}}$  and simplifies to set-up II if  $L_{\text{frame}} = l_{\text{frame}}$ .

### 3. Numerical shear frame tests on unit-cells

A unit-cell shown in Fig. 4a was designed to represent the periodic pattern of a plain weave composite with dry yarns [14]. The constitutive phases of the composite were glass fiber and polypropylene resin and their material properties are listed in Table 1. The volume fraction of the glass fiber in a fiber yarn was 70%. The homogenized elastic constants for a fiber yarn were taken from [14] as

$$E_l = 51.92 \text{ GPa}, \quad E_t = 21.97 \text{ GPa}, \quad \nu_{lt} = 0.2489$$

$$\nu_{tl} = 0.2143, \quad G_{lt} = 8.856 \text{ GPa}, \quad G_{tl} = 6.250 \text{ GPa}$$

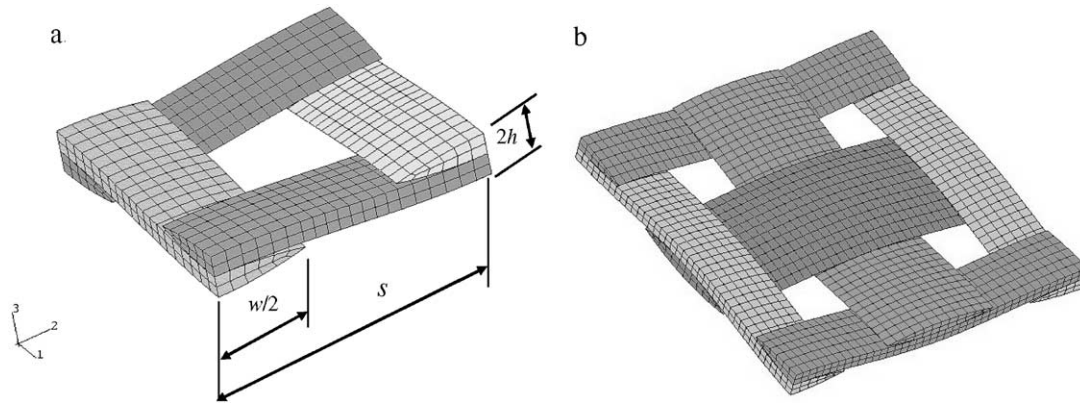


Fig. 4. (a) A unit cell for a plain weave composite. (b) An expanded unit-cell.

Table 1  
Material properties of E-glass/PP composite

Property	Unit	E-Glass	Polypropylene
Tensile modulus	GPa	73.1	1–1.4
Poisson's ratio	–	0.22	0.3
Axial shear modulus	GPa	30.19	
Density	kg/m <sup>3</sup>	2540	900

where  $l$  represented the longitudinal direction and  $t$  denoted the transverse direction of the yarn.

The unit cell was defined by four sinusoidal curves in terms of yarn width  $w$ , yarn spacing  $s$ , and fabric thickness  $h$ . The yarn cross-sections were approximated as circular arcs. The geometric characteristic values of  $w$ ,  $s$  and  $h$  were 3.72, 5.14 and 0.39 mm, respectively. The yarns of the plain weave composite were regarded as unidirectional fiber reinforced composite. Due to the voids between fibers, fiber yarns are not solid composites. Therefore, the homogenized elastic properties for fiber yarns should be much smaller than those of a single fiber, especially the transverse terms. Since our main purpose is to investigate the load normalization, the value of the elastic properties for dry yarns should not affect our results for normalization. Consequently, as an approximation, we will assume that the yarns have the same homogenized elastic properties as those of a single fiber.

The unit-cell was modeled with 3D continuum elements. The pin-joint net idealization was assumed along the four corners of the unit cell. Contact conditions were prescribed between the possible interlacing surfaces of the yarns under loading. The friction coefficient for the surface contact was taken to be 0.05 from previous experimental measurement [16]. To reflect the periodic boundary conditions in the shear frame tests, the cross-section and the split-surfaces of each yarn were constrained to be a flat surface and perpendicular to the in-plane surface during the trellising deformation.

For the sake of comparison, four identical unit-cells are combined to form an expanded unit-cell, as shown in Fig. 4b. The previous boundary conditions are also

imposed on the expanded unit-cell. Shear frame tests of set-up I under room temperature are now simulated on the two unit-cell models, respectively, by letting one corner of the unit-cells be clamped and pulling the diagonally opposite corner. The FEM simulation is carried out by prescribing displacements at the pulling corner. The loading force is obtained by adding the reaction forces at the clamped corner. The pulling rate in the experiments is not considered in the numerical tests since these are implicit static simulations.

The loads are normalized in two ways: by the unit-cell area and by the unit cell length. Fig. 5 shows the area-normalized load versus shear angle curves, and the length-normalized load versus shear angle curves are shown in Fig. 6. In Figs. 5 and 6, the plain solid line denotes the loads of the small unit-cell and the line with unfilled diamonds represents those of the expanded unit-cell. In Fig. 5, we can see that there is a large discrepancy between the two area-normalized loads after a shear angle of thirty degrees, and the difference has an increasing tendency with further shear deformation of the unit-cells. On the other hand, the difference between the two length-normalized loads remains in a small range during the entire deformation process, as shown in Fig. 6. The small discrepancy among the curves using

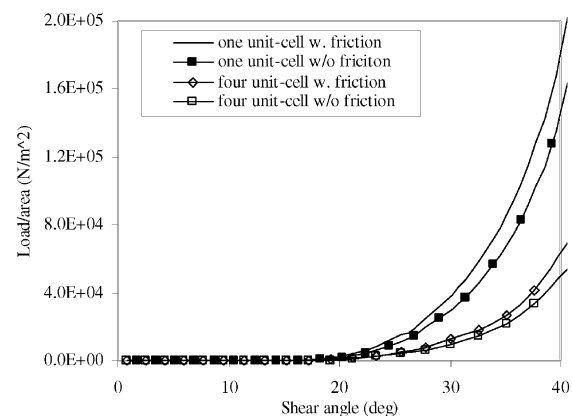


Fig. 5. Area normalization of loads in unit-cells.

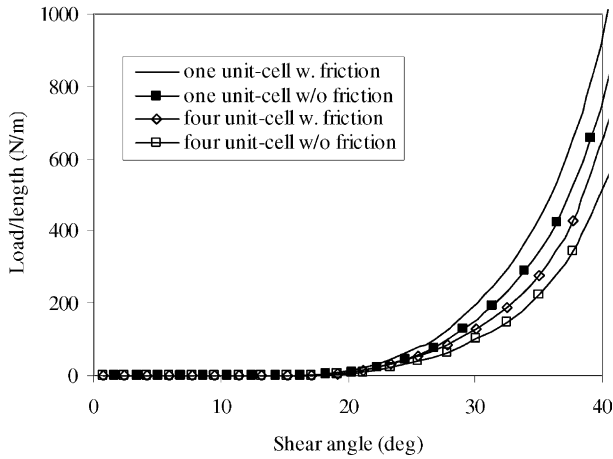


Fig. 6. Length normalization of loads in unit-cells.

the length normalization can be attributed to the thickness variation due to the compaction between yarns. The perfect length normalization obtained in Section 2 is based on the assumption that the thickness of the composite sheet does not change during the deformation.

To further investigate the normalization issue, we conducted numerical shear frame tests again on the two unit-cells with no friction between yarns. Results from the small unit-cell are represented by solid lines with black filled squares in both Figs. 5 and 6, and those from the expanded unit-cell are represented by solid lines with unfilled squares. It is observed again that, for the frictionless cases, the length-normalized load gives more consistent results for the two unit-cells as compared to the area-normalized load.

By deducting the loads without friction from those with friction, we obtain the load portion (we will therefore term it a friction load) resulting entirely from the friction. Again this friction load is normalized by area and length, respectively. Fig. 7 shows the area-normalized friction loads for the two unit-cells. As can be seen in Fig. 7, the area-normalized friction loads have a large

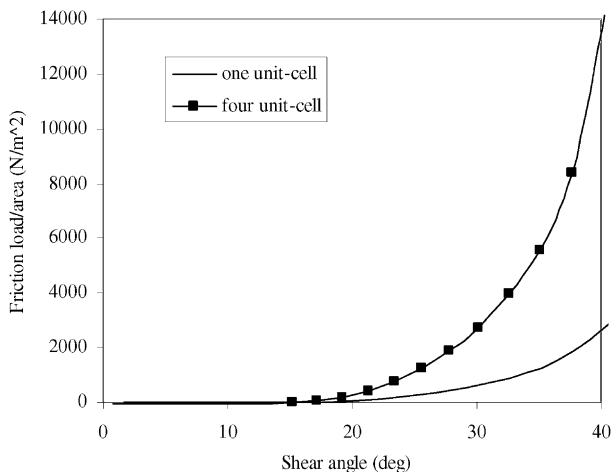


Fig. 7. Area normalization of friction load in unit-cells.

difference after a shear angle of 25 degrees. The difference becomes much larger with the increase of the shear angle. In contrast, the length-normalized friction loads are generally consistent for the two unit-cells during the shear forming process, as shown in Fig. 8. These FEM comparisons demonstrate that the length normalization is a more reasonable way than the area normalization to provide standard shear frame data for woven composites in trellising tests with set-up I. This is consistent with the finding from our theoretical analysis using the energy approach presented in Section 2.

#### 4. Numerical shear frame tests on woven composite sheets

The authors presented a material characterization method for plain weave composites and simulated the shear frame tests by using shell elements to model the composite sheet in [14]. As an improvement, a non-orthogonal material constitutive model was proposed in [15] so that the angle changes between yarns can be taken into account during the large shear deformation. The non-orthogonal model is used in this paper to model composite materials' behavior. Details of this non-orthogonal constitutive model can be found in [15] and the equivalent material constants needed for the constitutive model are listed in Table 2.  $D_{ij}$  in Table 2 are terms of the equivalent elastic matrix for a shell element under plane stress situation.

Numerical analyses using a commercial FEM package, ABAQUS/Standard, were conducted to simulate the shear frame tests with the two set-ups. Four-node shell elements (S4R) were used to model the fabric. According to the non-orthogonal constitutive model in [15], a user material subroutine was designed for ABAQUS/Standard and was incorporated into the four-node shell elements.

In set-up I, the shear frame was not modeled in the FEM analysis. Instead, boundary conditions with multi-

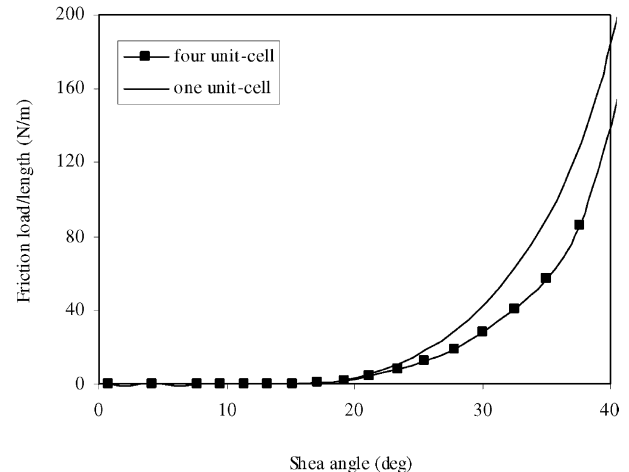


Fig. 8. Length normalization of friction load in unit-cells.

Table 2  
Material constants for non-orthogonal constitutive model

Equivalent Strain	$\varepsilon_i^+ \equiv \frac{\varepsilon_i +  \varepsilon_i }{2} = \begin{cases} \varepsilon_i & \varepsilon_i > 0 \\ 0 & \varepsilon_i \leq 0 \end{cases} \quad i = 1, 2$
$\bar{\varepsilon}^+$	$\bar{\varepsilon}^+ = \frac{2}{\sqrt{3}} \sqrt{(\varepsilon_1^+)^2 + (\varepsilon_2^+)^2 + (\varepsilon_1^+)(\varepsilon_2^+)}$
$D_{11}$ (MPa) $D_{22} = D_{11}$	$D_{11} = \frac{12600}{1 + e^{-280\bar{\varepsilon}^+}}$
$D_{12}$ (MPa) $D_{21} = D_{12}$	$D_{12} = 1100e^{-73\bar{\varepsilon}^+} \sin(80\bar{\varepsilon}^+ - 6.1) + 50$
$D_{33}$ (MPa)	$D_{33} \begin{cases} 3.08\gamma & \gamma < 0.3 \\ 3.15\gamma^3 + 15.79\gamma^2 - 5.0\gamma + 0.77 & \gamma \geq 0.3 \end{cases}$

point-constraints were imposed on the four edges of the composite sheet to make sure a pure shear deformation of the fabric. The composite sheets have three different fabric areas: 0.012 m<sup>2</sup> (110 mm×110 mm), 0.025 m<sup>2</sup> (158 mm×158 mm), and 0.044 m<sup>2</sup> (210 mm×210 mm).

In set-up II, the shear frame has a fixed size of 300 mm×300 mm. Composite sheets with the same size as the shear frame were cut off at four corners to generate three different central fabric areas of 0.012, 0.025 and 0.044 m<sup>2</sup>. Similar to the experiments, only the central dimension of the fabric will be used for normalization in set-up II. The shear frame was modeled by truss elements instead of beam elements to eliminate the effect of the frame on the trellising test results. Each edge of the frame can only rotate along the joints that connect to another frame edge. The shell elements were connected with the truss elements without slippage and separation by sharing the same nodes at the interfaces. One corner of the shear frame was clamped and the diagonally opposite corner was pulled to simulate the experimental shear frame tests, as in the cases of the unit cells. FEM simulations were carried out by prescribing displacements along the diagonal line at the pulling corner. The loading was obtained by collecting the reaction forces at the clamped corner. Fig. 9 shows the deformed meshes in the two set-ups. The contour plot of the shear strain in a composite sheet in set-up II is also shown in Fig. 9. It can be seen that the shear strain in the central area is reasonably uniform.

Fig. 10 shows the length-normalized load versus shear angle for set-up I. A perfect consistence of the loads with different fabric sizes is obtained by length normalization. This confirms our conclusion obtained from the theoretical energy analysis presented in Section 2. The shear frame tests were then applied to the fabric with set-up II. The length- and area-normalized load versus shear angle curves are shown in Figs. 11 and 12, respectively. In Figs. 11 and 12, the solid line with circles denotes the

load of the fabric of central area of 0.012 m<sup>2</sup>, the plain solid line is for the fabric of 0.025 m<sup>2</sup>, and finally the solid line with squares represents the fabric of 0.044 m<sup>2</sup>. As can be seen from Figs. 11 and 12, the length normalization provides a much better consistence of the load than the area normalization. This is somewhat in conflict with our conclusion obtained from the theoretical energy analysis in Section 2. However, in the numerical simulation of set-up II, the arm parts of composite fabrics were modeled with shell elements, which had the same material properties as those in the central square region. From the shear strain contour in Fig. 9, it is obvious that there exist non-negligible shear strains in the arm part from this FEM model, which contributes to the total load. Therefore, the load should be split into two parts: one deforms the central regions ( $P_{\text{center}}$ ), and the rest deforms the arm parts ( $P_{\text{arm}}$ ). In the real experimental composite fabrics, the arm parts either do not have any crossovers or are observed to be relatively free of deformation or compaction loads. Therefore, the work done by the pulling force is totally contributed to the deformation of the central region, as stated in Section 2. Consequently, we can choose the area of the central region as the effective area and only  $P_{\text{center}}$  should be used in the normalization.

The strain energy of each shell element in the central region and arm part region is recorded and added up to give the total strain energy in each region. We can then obtain the strain energy ratio between the two regions. Since we assume that the work done by the pulling load in the trellising deformation is totally converted to the strain energy of the fabric in our theoretical analysis (Section 2), the total pulling load in the numerical simulation should then be divided into two parts,  $P_{\text{center}}$  and  $P_{\text{arm}}$ , proportionally according to the strain energy ratio between the central square region and the arm parts of the composite fabric. Fig. 13 shows the area normalization of  $P_{\text{center}}$  that deforms the central part. As can be seen from Fig. 13, area normalization provides a perfect consistency for  $P_{\text{center}}$ . This conforms to the theoretical derivation for set-up II.

## 5. Shear frame tests on woven composite sheets

Experimental shear frame tests with set-up II on woven composite sheets were described in [11], in which the detailed experimental set-up was presented. The shear fixture used has a size of 300 mm×300 mm and is shown in Fig. 14. Composite sheets were clamped onto a shear frame by toggle clamps and a grooved surface to prevent slip, as shown in Fig. 14. The fabric was placed in the frame such that there was no slack and the yarns were oriented at  $\pm 45^\circ$  to the loading direction. The four corners of the fabric were cut off to generate experimental samples with various sizes. The effective size of

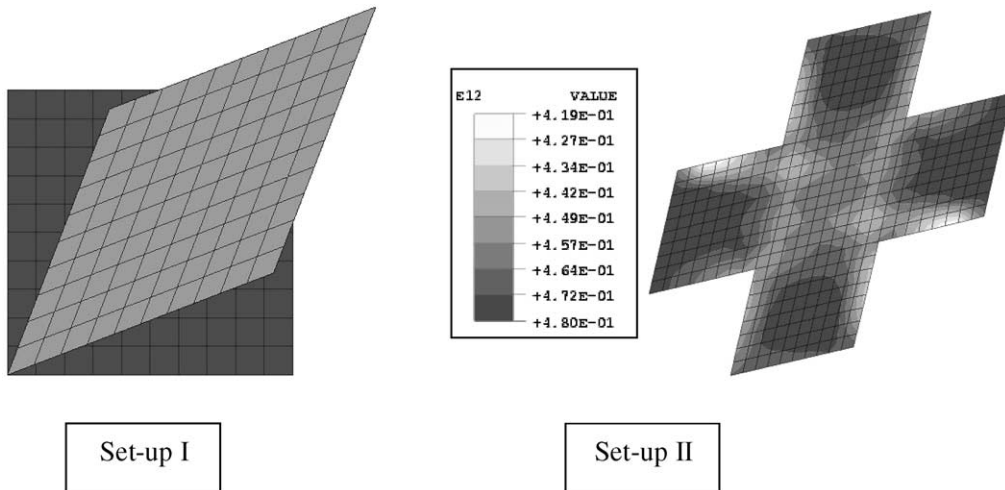


Fig. 9. Deformed fabric in numerical shear frame tests.

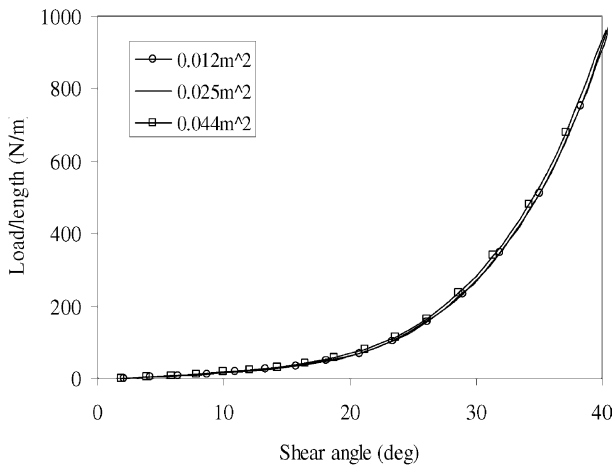


Fig. 10. Length-normalized simulation loads of set-up I.

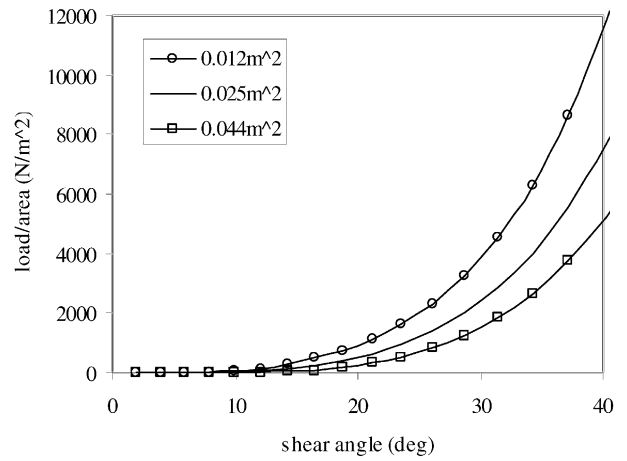


Fig. 12. Area-normalized total simulation loads of set-up II.

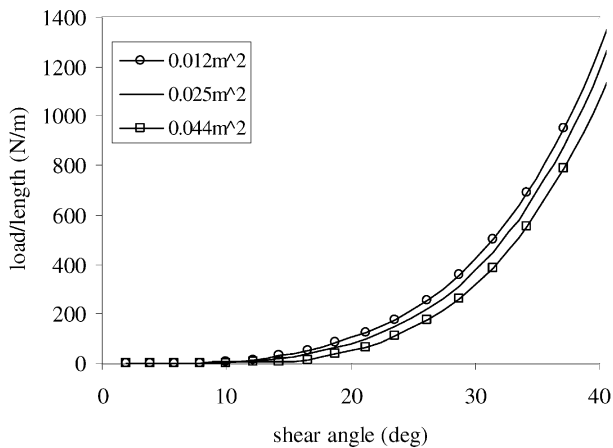


Fig. 11. Length-normalized total simulation loads of set-up II.

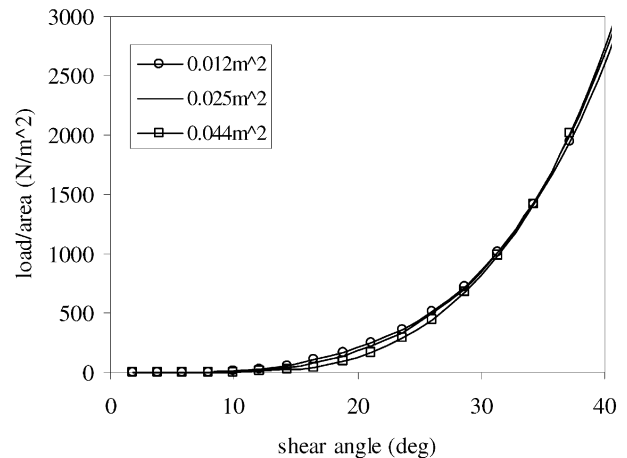


Fig. 13. Area normalization of  $P_{center}$  in set-up II.

the fabric was outlined by the black lines in Fig. 14. The shear frame tests were run at room temperature and at a crosshead rate of 50 mm/min with three different fabric central areas: 0.012 m<sup>2</sup> (110 mm×110 mm), 0.025m<sup>2</sup> (158 mm×158 mm), and 0.044 m<sup>2</sup> (210 mm×210 mm).

Four samples were prepared for each case. Fig. 15 shows the averaged experimental load versus displacement curves as well as the corresponding standard deviations for the three experimental cases. It is found from Fig. 15 that the experimental results were quite

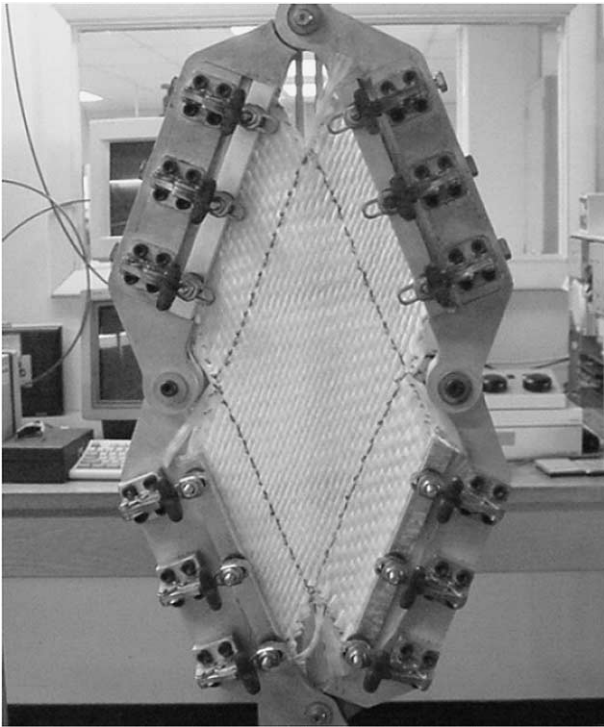


Fig. 14. Experimental set-up II for picture frame tests.

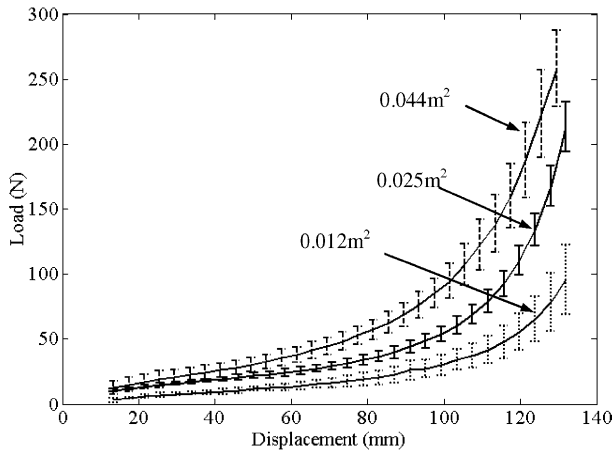


Fig. 15. Averaged experimental trellising results with error bars.

scattered. This can be attributed to several factors, such as the misalignment of fabric yarns, the variation of the tension force to keep the fabric out of slack, and the lack of fabric uniformity, etc.

The averaged loads versus shear angle curves for each experimental sample normalized by length and area are shown in Figs. 16 and 17, respectively. In Figs. 16 and 17, the solid line with circles represents the experimental sample of  $0.012 \text{ m}^2$ , the plain solid line is for the sample of  $0.025 \text{ m}^2$ , and finally the solid line with squares represents the sample of  $0.044 \text{ m}^2$ . As can be seen from Figs. 16 and 17, the area normalization results in a better consistence of the experimental loads in the trellising

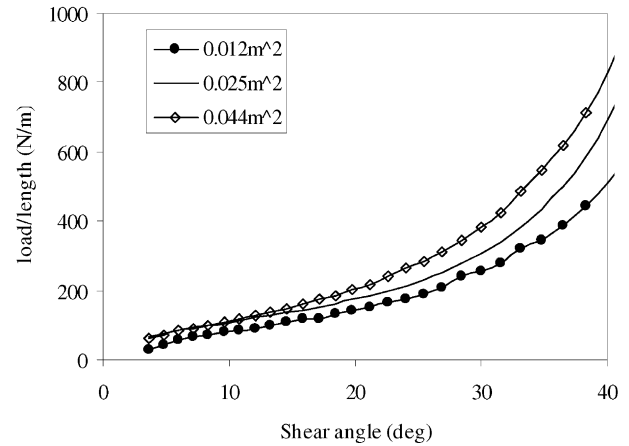


Fig. 16. Length normalization of averaged experimental loads in set-up II.

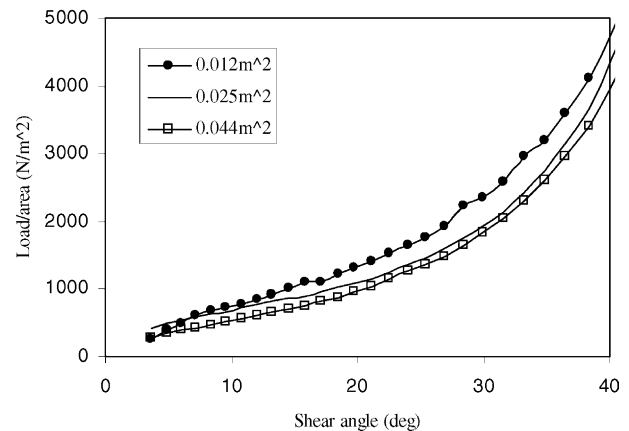


Fig. 17. Area normalization of averaged experimental loads in set-up II.

tests with set-up II. Again, this is consistent with the conclusion obtained from our theoretical analysis using the energy approach in Section 2 and the FEM simulations of setup II in Section 4. Nevertheless, the length normalization also can provide a good consistence of the averaged loads at low shear angles, as shown in Fig. 16. The possible reason behind this phenomenon will be given in Section 6.

## 6. Discussion

As presented in Figs. 16 (length normalization) and 17 (area normalization), experimental shear frame tests of set-up II are closer to the area normalization than the length normalization, while the theoretical analysis and numerical simulations suggested an area normalization (see Section 2). The deviation of test results from perfect area normalization is partially due to the large scattering of the experimental data and partially attributed to the force contribution from the arm parts of the composite sheets. Significant improvement on repeatability

can be achieved through mechanical conditioning, i.e., shearing the specimen in the frame several times to align the yarns, as suggested in [17]. This will be the major focus of our future experiments. In this paper, we will concentrate our discussion mainly on the load contribution from the arm parts and experimental set-ups beneficial to the benchmark tests for woven composites.

### 6.1. Effect of load contribution from the arm parts

The theoretical derivation on load normalization presented in Section 2 is based on the assumption that the arm parts have no contribution to the total load. This is an ideal extreme. Another extreme is that the arm parts have the same shear strain distribution as that in the central region. For this extreme idealization, referring to Fig. 2, we have for general set-ups that

$$\begin{aligned} \frac{W}{w} &= \frac{\bar{P}\Delta_p}{\bar{p}\delta_p} = \frac{A_{\text{ENTIRE-FABRIC}}}{A_{\text{entire-fabric}}} \\ &= \frac{L_{\text{fabric}}^2 + 2(L_{\text{frame}} - L_{\text{fabric}})L_{\text{fabric}}}{l_{\text{fabric}}^2 + 2(l_{\text{frame}} - l_{\text{fabric}})l_{\text{fabric}}} \end{aligned} \quad (12)$$

Substitution of Eq. (7) into (12) brings us to

$$\frac{\bar{P}}{\bar{p}} = \left[ \frac{L_{\text{fabric}}^2 + 2(L_{\text{frame}} - L_{\text{fabric}})L_{\text{fabric}}}{l_{\text{fabric}}^2 + 2(l_{\text{frame}} - l_{\text{fabric}})l_{\text{fabric}}} \right] \frac{l_{\text{frame}}}{L_{\text{frame}}} \quad (13)$$

The above relation is quite different from Eq. (11) in which zero load contribution from the arm parts is assumed.

Let us consider a special case where we have two tests of the same frame size, but one test with cut-off fabric and another test with full fabric. i.e.,  $L_{\text{frame}} = l_{\text{frame}}$  and  $l_{\text{fabric}} = l_{\text{frame}}$  and we define  $\alpha = L_{\text{fabric}}/L_{\text{frame}}$  ( $\alpha \leq 1$ ), then with the assumption of zero contribution from the arm parts, Eq. (11) can be simplified as,

$$\frac{\bar{P}}{\bar{p}} = \frac{L_{\text{fabric}}^2}{L_{\text{frame}}^2} = \alpha^2 \quad (14)$$

Similarly, with the assumption of equal load contribution rate from the arm parts, Eq. (13) can be simplified as,

$$\frac{\bar{P}}{\bar{p}} = \frac{L_{\text{fabric}}^2 + 2(L_{\text{frame}} - L_{\text{fabric}})L_{\text{fabric}}}{L_{\text{fabric}}^2} = 2\alpha - \alpha^2 \quad (15)$$

By choosing  $\alpha$  to be the  $x$ -variable and  $\bar{P}/\bar{p}$  as the  $y$ -variable, we represent Eq. (14) by a dashed curve and Eq. (15) by a solid curve, respectively, in Fig. 18. The area encircled by these two curves corresponds to an intermediate load contribution rate from the arm parts.

We have presented the experimental results of three cut-off cases in Section 5: 110 mm  $\times$  110 mm

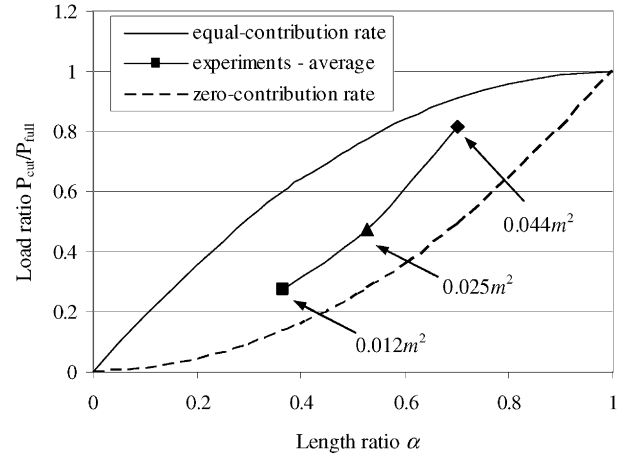


Fig. 18. Investigation on load contribution from arm parts at 35° shear deformation.

( $\alpha = 110/300 = 0.3667$ ), 158 mm  $\times$  158 mm ( $\alpha = 158/300 = 0.5267$ ), and 210 mm  $\times$  210 mm ( $\alpha = 210/300 = 0.7$ ). Some corner cut-off is typically needed to allow rotation of the hinges and prevent immediate wrinkling of fabrics. Consequently, it is very hard to experimentally obtain the results for a full size fabric (300 mm  $\times$  300 mm, without cut-off). To circumvent this difficulty, the experimental loads of the full size fabric are obtained from the numerical simulation using the model in Fig. 9a. An experimental curve under 35° shear deformation is presented in Fig. 18 by a solid line with filled data points, in which the square represents the 110 mm  $\times$  110 mm test, the triangle represents the 158 mm  $\times$  158 mm test, and the rhombus denotes the 210 mm  $\times$  210 mm test. The experimental curve is positioned between the theoretical curves, as shown in Fig. 18. Obviously, the experimental force contribution from the arm parts in cut-off samples are between these two ideal extremes. Fig. 18 can be used to qualitatively evaluate the experimental contribution from the arm parts.

### 6.2. Experimental set-ups for benchmark tests of woven composites

When it comes to the general set-ups (two different shear frames sizes and the fabric in each frame have different cut-offs), the loads usually fall into neither length normalization nor area normalization no matter how much the arm part contribution is, as demonstrated by Eqs. (11) and (13), respectively. This will complicate the setting-up of the benchmark tests for woven composites which is currently being undertaken by the ‘authors’ and other ‘researchers’.

Let us consider a special set-up where  $L_{\text{fabric}}/L_{\text{frame}} = l_{\text{fabric}}/l_{\text{frame}} = \alpha$  ( $\alpha \leq 1$ ) and  $L_{\text{frame}}$  is not necessarily equal to  $l_{\text{frame}}$ , then with the assumption of zero contribution from the arm parts, Eq. (11) can be simplified as,

$$\frac{\bar{P}}{\bar{p}} = \left[ \frac{L_{\text{fabric}}/L_{\text{frame}}}{l_{\text{fabric}}/l_{\text{frame}}} \right] \frac{L_{\text{fabric}}}{l_{\text{fabric}}} = \left[ \frac{\alpha}{\alpha} \right] \frac{L_{\text{fabric}}}{l_{\text{fabric}}} = \frac{L_{\text{fabric}}}{l_{\text{fabric}}} \quad (16)$$

which gives length normalization for loads.

Similarly, with the assumption of *equal* load contribution rate from the arm parts, Eq. (13) can be simplified as,

$$\begin{aligned} \frac{\bar{P}}{\bar{p}} &= \left[ \frac{L_{\text{fabric}}/L_{\text{frame}} + 2(1 - L_{\text{fabric}}/L_{\text{frame}})}{l_{\text{fabric}}/l_{\text{frame}} + 2(1 - l_{\text{fabric}}/l_{\text{frame}})} \right] \frac{L_{\text{fabric}}}{l_{\text{fabric}}} \\ &= \left[ \frac{\alpha + 2(1 - \alpha)}{\alpha + 2(1 - \alpha)} \right] \frac{L_{\text{fabric}}}{l_{\text{fabric}}} = \frac{L_{\text{fabric}}}{l_{\text{fabric}}} \end{aligned} \quad (17)$$

Again, we have arrived at the length normalization.

Eqs. (16) and (17) suggest that, for a special set-up  $L_{\text{fabric}}/L_{\text{frame}} = l_{\text{fabric}}/l_{\text{frame}}$ , trellising loads should be normalized by the central region length under the assumptions of *zero* or *equal* contribution from the arm parts. This will be beneficial to our benchmarking task.

The load contribution rate from the arm parts is dependent on how much compaction occurs in the arm parts and how the overall restriction of the yarns in both the arms and the center region affect the compaction loads. If the load contribution rate from the arm parts is not equal to that in the central region, the situation will become complicated again. Suppose that the load contribution rates from the arm parts are  $\Gamma$  for the set-up of  $L_{\text{fabric}} - L_{\text{frame}}$  and  $\gamma$  for  $l_{\text{fabric}} - l_{\text{frame}}$ , respectively, then Eq. (17) should be modified as,

$$\frac{\bar{P}}{\bar{p}} = \left[ \frac{\alpha + 2\Gamma(1 - \alpha)}{\alpha + 2\gamma(1 - \alpha)} \right] \frac{L_{\text{fabric}}}{l_{\text{fabric}}} \quad (18)$$

We can have length normalization only if  $\Gamma = \gamma$ , which is very hard to maintain in experiments.

## 7. Conclusions

Normalization of loads in shear frame tests of plain weave composites is investigated in this paper. A typical experimental setup is shown in Fig. 14. Theoretical analysis and numerical simulations show that the normalization method depends on the set-up of the shear frame tests and the assumptions about the load contribution from the arm parts of samples with corner cut-offs. Length normalization should be used in order to obtain consistent material behavior of plain weave composites if the shear frame tests are carried out with various frame sizes and the composite sheet fills up the frames completely. To compare combined differences in shear frame size and specimen size, load normalization can be achieved through Eq. (11) under the assumption of zero load contribution from the arm parts or through Eq. (13) by assuming that the arm parts have the same

load contribution rate as that in the central region. It must be noted that all cases reduce to length normalization [Eq. (18)] IF the same ratio of fabric length to frame length is used and IF the ratio of load contribution rate of the arm parts to that of the central region is the same ( $\Gamma = \gamma$ ).

The effect of the arm parts on the total load complicates the material characterization of woven composites. Shear frame tests similar to set-up I are strongly recommended in order to provide an accurate material characterization of woven composites. Unfortunately, some corner cut-offs are typically needed to allow rotation of the hinges and to prevent immediate wrinkling of fabrics. Thus the effect from the corner cut-off (i.e., the effect of the arms) should be minimized using small cut-offs. Another possible way to eliminate the contribution from the arm parts is by, in each arm part, pulling out all the fiber yarns, which are not clamped to the shear frame. In this case, care should be taken to ensure that the clamped yarns are not slack. The conclusion obtained in this work is beneficial to the benchmark tests for woven composites. Benchmarking is crucial in identifying and correlating various materials characterization tests for formability and forming of composite materials. Further efforts are ongoing in order to set up benchmark tests for woven composite materials.

## Acknowledgements

The authors would like to thank the NSF Division of Design, Manufacture, and Industrial Innovation (DMI-9900185) and Ford Motor Company for their support of this research. The helpful discussions with Prof. Tongxi Yu at HKUST are greatly appreciated.

## References

- [1] Boisse P, Borr M, Buet M, Cherouat A. Finite element simulations of textile composite forming including the biaxial fabric behavior. *Composites Part B-Engineering* 1997;28:453–64.
- [2] Potter KD. The influence of accurate stretch data for reinforcements on the production of complex structural moldings part I: deformation of aligned sheets and fabrics. *Composites* 1979;11: 161–7.
- [3] Potter K. Influence of the detailed structure of two variants of non-crimped carbon fabric on the drape properties. *Advanced Composites Letters* 2002;11:285–92.
- [4] Potter K. Bias extension measurements on cross-plyed unidirectional prepreg. *Composites Part A* 2002;33:63–73.
- [5] Buckenham P. Bias-extension measurements on woven fabrics. *Journal of the Textile Institute* 1997;88:33–40.
- [6] McBride TM, Chen J. Unit-cell geometry in plain-weave fabrics during shear deformation. *Composites Science and Technology* 1997;57:345–51.
- [7] Chen J, Lussier DS, Cao J, Peng XQ. Materials characterization methods and material models for stamping of plain woven composites. *International Journal of Forming Processes* 2002;4(3–4).

- [8] McGuinness GB, Bradaigh CMO. Development of rheological models for forming flows and picture-frame shear testing of fabric reinforced thermoplastic sheets. *Journal of Non-Newtonian Fluid Mechanics* 1997;73:1–28.
- [9] McGuinness GB, Brádaigh CMO. Characterization of thermoplastic composite melts in rhombus-shear: the picture frame experiment. *Composites Part A* 1998;29:115–32.
- [10] Nguyen M, Herszberg I, Paton R. The shear properties of woven carbon fabric. *Composite Structures* 1999;47:767–79.
- [11] Lussier D, Chen J. Material characterization of woven fabrics for thermoforming of composites. In: *Proceedings of the 15th Technical Conference of American Society for Composites*, College Station, TX, 2000. p. 301–10.
- [12] Long AC. An iterative draping simulation based on fabric mechanics. In: *Proceedings of the 4th International ESAFORM Conference on Material Forming*, Liège, Belgium, 2001. p. 99–102.
- [13] Harrison P, Clifford MJ, Long AC, Rudd CD. Constitutive modeling of impregnated continuous fiber reinforced composites—micromechanical approach. *Plastics Rubber and Composites* 2002;31:76–86.
- [14] Peng XQ, Cao J. A dual homogenization and finite element approach for material characterization of textile composites. *Composites Part B* 2002;33:45–56.
- [15] Xue P, Peng XQ, Cao J. A non-orthogonal constitutive model for characterizing woven composites. *Composites Part A* 2003;34:183–93.
- [16] Prodromou AG, Chen J. On the relationship between shear angle and wrinkling of textile composite performs. *Composites Part A* 1997;28:491–503.
- [17] Chen J, Lussier DS, Sherwood A, Cao J, Peng XQ. The relationship between materials characterization methods and material models for stamping of woven fabric/thermoplastic composites. In: *Proceedings of the 4th international ESAFORM conference on material forming*, Liège, Belgium, 2001, p. 127–30.